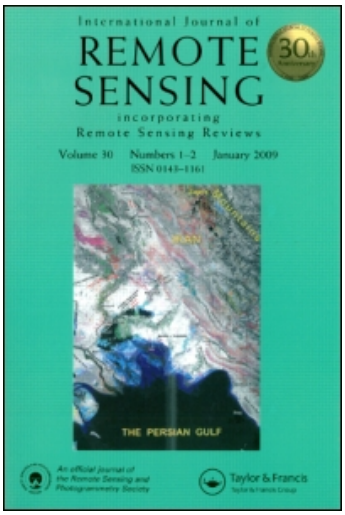

International Journal of Remote Sensing
Publication details, including instructions for authors and subscription information:
http://www.informaworld.com/smpp/title~content=t713722504

Application of the Crosta technique for alteration mapping of granitoidic rocks using ETM+ data: case study from eastern Tauride belt (SE Turkey)

D. Aydal [a]; E. Arda [a]; Ö. Dumanlilar [b]
[a] Ankara University, Faculty of Engineering, Geological Engineering Department, Beevler-Ankara, Turkey [b] Demir Export, Koçhan, Kzlay-Ankara, Turkey

Online Publication Date: 01 January 2007

To cite this Article Aydal, D., Arda, E. and Dumanlilar, Ö.(2007)'Application of the Crosta technique for alteration mapping of granitoidic rocks using ETM+ data: case study from eastern Tauride belt (SE Turkey)',International Journal of Remote Sensing,28:17,3895 — 3913

To link to this Article: DOI: 10.1080/01431160601105926

URL: http://dx.doi.org/10.1080/01431160601105926

International Journal of Remote Sensing
Vol. 28, No. 17, 10 September 2007, 3895–3913

Taylor & Francis
Taylor & Francis Group

Application of the Crosta technique for alteration mapping of granitoidic rocks using ETM+ data: case study from eastern Tauride belt (SE Turkey)

D. AYDAL*†, E. ARDA1† and Ö. DUMANLILAR‡
†Ankara University, Faculty of Engineering, Geological Engineering Department, 06100, Beşevler-Ankara, Turkey
‡Demir Export, Koçhan, Kızılay-Ankara, Turkey

(*Received 11 October 2005; in final form 7 November 2006*)

The present study particularly focuses on the determination of alteration products of the granitoid associations by remote sensing techniques. Widespread magmatism has occurred in the Malatya-Elazığ area of the eastern Tauride belt in south east Turkey as a consequence of plate convergence and continental collision. The development of the magmatism in the study area can be subdivided into two separate phases, the Baskil and the Bilaser Tepe complexes. Based on the petrographic and bulk-rock geochemical data, the Baskil granitoids are classified as quartz-diorite, quartz-monzodiorite and tonalite, whereas the Bilaser Tepe granitoids are classified as granodiorite and dacite-porphyry. Both the Baskil and Bilaser Tepe granitoids have peraluminous and metaluminous compositions. The Crosta method is found to be very useful for enhancing the altered areas with hydroxyl and iron oxide minerals. The Crosta method is applied to six (1, 2, 3, 4, 5 and 7) and two sets of four (1, 3, 4, 5 and 1, 4, 5, 7) bands of ETM+ data. However, the areas with potassic, phyllic, argillic and propylitic alteration zones are enhanced much better by using six bands of Landsat 7 ETM+ data. The alteration differences of these two magmatic groups are also tested with the Crosta technique using four band combinations. Although no distinct difference is observed on the hydroxyl image, a clear difference is observed between the two magmatites on the iron oxide image. The present study shows that the Crosta technique is not only generating hydroxyl and iron oxide images, but also differentiates between two magmatite groups of different ages and genesis.

1. Introduction

The study area, situated to the south of Baskil (42.535–42.720° N; 47.700–49.000° E), is dominated by Late Cretaceous magmatic rocks (Asutay 1985), and Plio-Quaternary and Quaternary sedimentary units (see figure 1). The Late Cretaceous granitoid associations in the Malatya-Elazığ area exhibit calc-alkaline and tholeiitic major oxide trends. In the study area, Baskil magmatites are represented by quartz-diorite, quartz-monzodiorite, and tonalite. We will refer to these as the Baskil granitoids.

Granitic rocks, defined by earlier researchers as belonging to later phases of the Baskil magmatites, were re-evaluated as the Bilaser Tepe magmatites, and were

*Corresponding author. Email: aydal@eng.ankara.edu.tr

International Journal of Remote Sensing
ISSN 0143-1161 print/ISSN 1366-5901 online © 2007 Taylor & Francis
http://www.tandf.co.uk/journals
DOI: 10.1080/01431160601105926

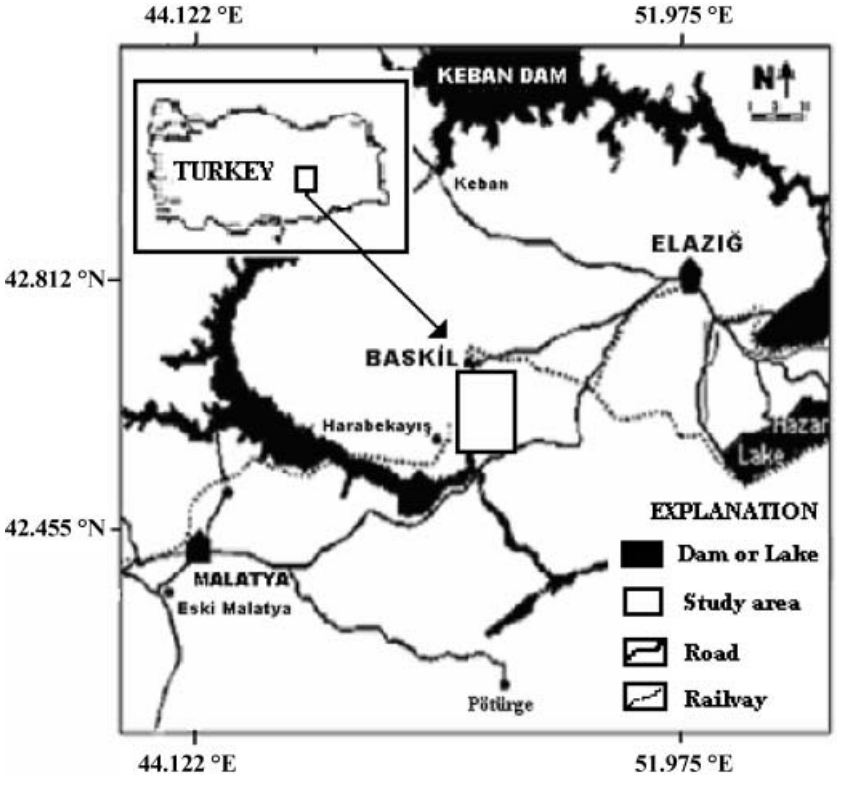

Figure 1. Location of the study area.

considered as a separate phase throughout the present study on the basis of field, petrographical, and geochemical data (Dumanlılar *et al*. 2005a, 2005b). The Bilaser Tepe magmatites have intrusive contacts with the Baskil magmatites and comprise five different phases: granite, granodiorite, granite-porphyry, granodiorite-porphyry and dacite-porphyry.

According to Lowell and Guilbert's (1970) definition, potassic, phyllic and propylitic alteration in granodiorites and phyllic alteration in granite-porphyry were detected. Finally, the last member of the Bilaser Tepe magmatites, dacite-porphyry displays phyllic alteration. Additionally, quartz-serisite-carbonate alteration was detected in the inner part of the diorites, as well as around the auriferous quartz veins located between the diorite-granodiorite contacts (Dumanlılar 2002).

Landsat data has been used for the last two to three decades in arid and semi-arid environments to locate the areas of iron oxides and/or hydrous minerals that might be associated with hydrothermal alteration zones of ore deposits (Abrams *et al*. 1983, Kaufman 1988, Tangestani and Moore 2001).

The host rocks that contain ore deposits and/or enriched in ore minerals of hydrothermal origin always display the end-products of interaction with the hydrothermal fluids that could change the ore minerals and chemical composition of the rocks and cause the deposition of the ore and related hydrothermal minerals (Rutz-Armenta and Prol-Ledesma 1998).

Almost all porphyry deposits show a well-developed zonal pattern of mineralization and wallrock alteration, as seen in Baskil and its environs. This

can be described by broad variations in major oxides and trace element concentrations. These elemental compositions in turn reflect variations in the mineralogical composition of the altered zones. Supergene alteration results in the formation of extensive iron oxide minerals, giving characteristic chestnut reddish and/or yellowish colour to the altered rocks. These alteration minerals can be detected by remote sensing techniques.

Principal component analysis is commonly used for alteration mapping in metallogenic provinces (Abrams *et al.* 1983, Kaufman 1988, Loughlin 1991, Bennett *et al.* 1993, Tangestani and Moore 2001, Ranjbar *et al.* 2002). The Crosta technique is known as a feature oriented principal components selection. Through the analysis of the eigenvector values, it allows identification of the principal components that contain spectra information about specific minerals, as well as the contribution of each of the original bands to the components in relation to the spectral response of the materials of interest. This technique indicates whether the materials are represented with bright or dark pixels in the principal components according to the magnitude and sign of the eigenvectors loadings. This technique can be applied to four and six selected bands of TM data (Crosta and Moore 1989, Rutz-Armenta and Prol-Ledesma 1998).

2. Geological Setting

Numerous studies of the geology, tectonics, and petrographical and petrological aspects of the study area and environs have been undertaken in the past (Yazgan 1981, 1984, Asutay and Turan 1986, Asutay 1988, Yazgan and Chessex 1991, Beyarslan 1991, Akgül 1991, Herece *et al.* 1992, Turan *et al.* 1995, Dumanlılar 1993, 1998, 2002, Dumanlılar *et al.* 1999, Dumanlılar *et al.* 2005a, 2005b).

The Baskil and Bilaser Tepe magmatic rocks were first defined by Perinçek (1979). Various researchers who had worked elsewhere in the eastern Taurides defined them collectively as the Yüksekova Complex (Perinçek 1979, Turan 1984, Bingöl 1988, Dumanlılar 1998). The same magmatic rocks were named the Baskil Magmatites by Asutay (1985), the Baskil Magmatic Rocks by Yazgan *et al.* (1987) and the Elazığ Magmatites by Akgül and Bingöl (1997). Herece *et al.* (1992) suggested that the Late Cretaceous magmatites cropping out in the vicinity of Elazığ developed during two different time intervals: the first was defined as the Baskil Magmatic Complex, and the second as the Pertek Magmatic Complex. Throughout this work, magmatic rocks near Baskil have been mapped as two distinct units, namely the Baskil and the Bilaser Tepe Granitoids.

2.1 *Baskil magmatic rocks*

In the study area, the first phase of the Baskil magmatic rocks is represented by dioritic rocks. The subsequent acidic phase is of tonalitic composition. The studies of Akgül and Bingöl (1997) near Keban, and those of Dumanlılar (1998) near Malatya, proposed that magmatism was initiated as a basic phase and later shifted to an acidic phase. Asutay (1985) who originally examined magmatic rocks near Baskil, stated that regional magmatic rocks show gradual transitions to each other and divided them into four groups: (1) diorite-monzodiorite, (2) a transition group (quartz–diorite), (3) granodiorite-tonalite, and (4) monzonite. He also regarded andesitic and basaltic volcanic rocks as the final products of the Baskil Magmatism.

Quartz-diorite crops out over an area stretching from the southern part of the Badem Tepe-Hemik Tepe line to Cansızhimik Mahallesi, and is surrounded by units of the Bilaser Tepe magmatites as shown in figure 2. Quartz-monzodiorite crops out around Bejikan Ziyareti Tepe. It has a lighter green colour than the quartz-diorite and is characterized by a coarser grain size. Tonalite, exposed in the extreme northwestern part of the study area, is distinguished by its greyish dirty-white colour and coarse (up to 1 cm) grain size, with the elliptical or rounded quartz grains having a vitreous luster.

The modal mineralogical compositions of selected samples from the Baskil granitoids are listed in table 1. Petrographical and modal mineralogical investigations demonstrate that the Baskil granitoids are composed of quartz-diorite, quartz-monzodiorite and tonalite. The quartz-diorite and quartz-monzodiorite are grouped as dioritic rocks and will be referred to as dioritic rocks in subsequent sections. The modal mineralogical analysis shown in table 1 presents quartz, plagioclase and chlorite as the main components of the tonalite volume.

2.2 *Bilaser Tepe magmatic rocks*

As stated earlier, the Bilaser Tepe magmatites have intrusive contacts with the Baskil magmatites and comprise five different phases: granite, granodiorite, granite-porphyry, granodiorite-porphyry and dacite-porphyry. The outermost granite crops out over an area extending from the northern side of the Badem

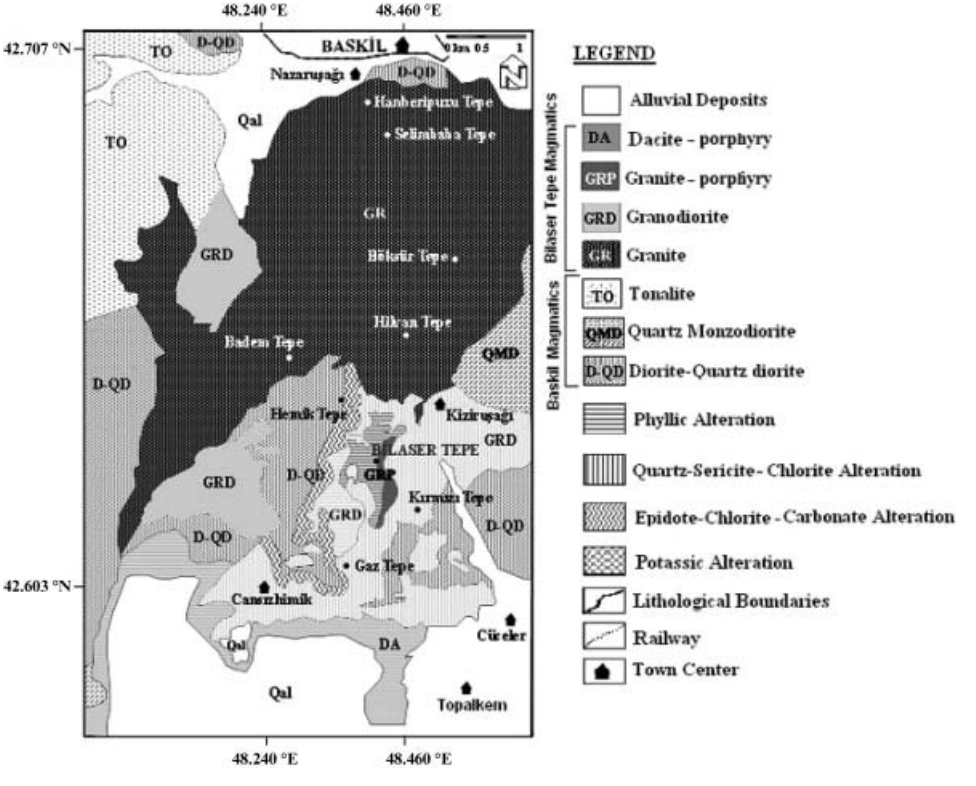

Figure 2. Simplified lithological and alteration map of the study area.

Table 1. Modal mineralogical analysis of the Baskil magmatites (dioritic rocks and tonalite).

Sample no.	Rock name	Components (%)					
		Quartz	Alkali feldspar	Plagioclase	Hornblende	Chlorite	Oxides
BY10	Dioritic	1.2	–	54.6	37.4	–	6.8
BY11	rocks	4.2	–	51.5	39.1	–	5.2
T22		11.8	–	53.7	32.0	2.2	0.3
KA8		3.7	8.5	42.9	43.0	1.9	–
KA7		4.9	7.1	38.9	46.8	2.3	–
T28	Tonalite	43.9	–	49.85	–	6.25	–
T21		40.1	–	54.1	–	5.8	–
T24		58.9	–	37.7	–	2.6	0.8

Tepe-Hemik Tepe-Kiziruşağı Mahallesi line of the Baskil flatland (as shown in figure 2). It is easily distinguished by its typical pinkish colour. Rocks of this unit are characterized by their N 80° E/30° NE joint set, and by their pinkish-white arenated appearance. Aplite veins 10 to 50 cm thick occur with variable orientations in these granites.

At Bilaser Tepe, granite-porphyry occurs at the centre and grades outwards to granodiorite with a gradual transition between these rock types. Granodiorite crops out to the south of Kiziruşağı Mahallesi and to the north of Cansızhimik Mahallesi (as shown in figure 2). This unit, which has intrusive contacts with the diorite and granite of the Baskil magmatites, occasionally occurs as 1 to 20 m thick veins within them. It is greyish green in outcrop and has a finer-grained texture than the other units of the Bilaser Tepe magmatites. The greyish-white granite-porphyry forms the central part of the Bilaser Tepe magmatites and is easily distinguished from the other units by its higher quartz content and lack of mafic minerals. Granodiorite-porphyry crops out in a narrow zone to the northwest of Kiziruşağı Mahallesi (see figure 2). The mafic mineral content of this unit is higher than that of the granodiorite unit, and other components (except for alkali feldspar) have a smaller grain size. Alkali feldspar reaches up to 2 cm in size.

The east to west trending dacite-porphyry, the latest phase of the Bilaser Tepe magmatites, crops out in the south of Cansızhimik Mahallesi. The dacite-porphyry, the youngest unit in the study area, shows a gradual transition to granodiorite of the Bilaser Tepe magmatites to the north, while having intrusive contacts with units of the Baskil magmatites to the west. The eastern margin is overlain by younger sediments. The dacite-porphyry has intrusive contacts with the Sağdıçlar Formation (Late Campanian-Early Maastrichtian), consisting of alternating mudstone, siltstone, and limestone, with volcanic claystone along their southern margins (outside the study area).

The modal mineralogical compositions of selected samples from the Bilaser Tepe granitoids are listed in table 2. Petrographical and modal mineralogical investigations demonstrate that these rocks comprise granite and granodiorite. In the study area, two types of granitic rocks can be distinguished on the basis of their textural features: granite and granite-porphyry. Granite and granite-porphyry are grouped as granitic rocks and thus will be referred to as granite in the following sections. The modal mineralogical analysis (table 2) of the granitic rocks reveals that

Table 2. Modal mineralogical analysis of the Bilaser Tepe granitic rocks (granite and granodiorite).

Sample No	Rock name	Components (%)					
		Quartz	Alkali feldspar	Plagioclase	Hornblende	Biotite	Oxides
BY16	Granite	23.5	44.9	24.8	6.8	–	–
N18		29.2	44.7	24.2	1.1	0.8	–
BY13		17.4	38.6	33.3	10.2	–	0.5
N2		44.0	24.4	28.0	3.6	–	–
D29		25.0	24.0	41.0	10.0	–	–
N2-1		42.0	23.6	30.4	4.0	–	–
TS7-2P		57.8	24.5	16.5	–	1.2	–
TS2-P33		53.4	26.5	18.4	–	1.4	0.3
TS2-P26		47.6	32.4	19.6	–	0.4	–
TS3-P10		45.2	34.8	19.6	–	0.4	–
BF-5	Granodiorite	28.5	21.4	39.6	–	7.9	2.6
TS3-P6		25.3	19.9	39.7	–	14.5	0.6
TS-31		22.2	22.8	40.0	5.4	8.6	1.0
KA-6		27.2	19.8	44.2	6.3	2.5	–
N1		21.7	20.1	40.4	7.4	7.8	2.6
TS-17		28.0	21.2	41.8	1.8	6.6	0.6
TS-35		27.6	18.7	38.4	2.4	12.4	0.5

quartz, alkali feldspar, plagioclase, hornblende, and biotite, with relatively lesser amounts of oxides make up the significant percentages of the granite volume.

3. Data analysis

Landsat 7 ETM+ data (173/33 path/row, acquisition date 10 December 2003) of the Baskil area is used for this study. The cloud free image is geometrically corrected by using control points from 1 : 25000 scaled topographic sheets. Baskil (Elazığ) and its environs was extracted as one sub-scene (about 70 km^2) from the Landsat 7 ETM+ data. Several image-enhancement techniques such as decorrelation stretching, filtering, algebraic processes (addition, extraction, subtraction, division) and principal component analysis (PCA) were applied to the sub-image, and thematic evaluations were made in addition to the application of Crosta techniques to this imagery. The results of the studies related to the image-enhancement techniques have been prepared as a separate research paper; therefore, the results are not discussed in this paper in detail.

The outcome of the other applications performed by the present authors and relevant previous studies (Crosta and Moore 1989, Loughlin 1991, Tangestani and Moore 2000, Ranjbar *et al.* 2004) lead to the band combination chosen for this study.

It is conventionally known that clay minerals exhibit strong absorption in Landsat band 7 (2.08–2.35 μm) and high reflectance in band 5 (1.55–1.75 μm). On the other hand, the use of the ratio of these bands (7/5 ratio) has enhanced the final image clay minerals. Similarly, the 7/1 band ratio is preferred for hydroxyl alteration and the 3/1 band ratio preferred for iron oxide alteration (Sabins 1997, 1999, Drury 2001). It is possible to conclude that bands 1, 3, 5 and 7 of the Landsat 7 ETM+ data are widely used for geological studies. This is probably the reason for

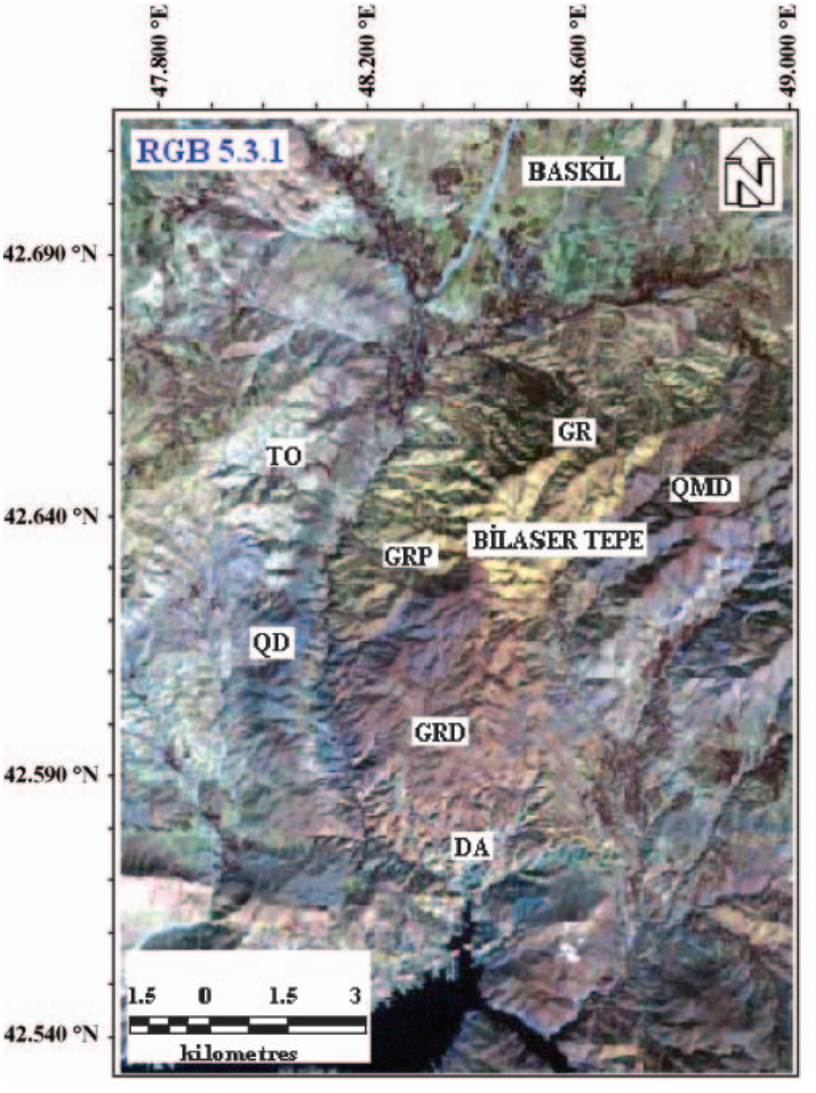

Figure 3. RGB 531 composite image of the sub-scene of the study area. All principal component transformations are made by using the six bands (1, 2, 3, 4, 5 and 7) of Landsat 7 ETM+. (Abbreviations: GR – Granite, GRD – Granodiorite, GRP – Granite-porphyry, TO – Tonalite, QD – Quartz-diorite, QMD – Quartz-monzodiorite, DA – Dacite-porphyry.)

their use in the Crosta technique. More specifically, RGB 731, RGB 754, RGB 753 and RGB 531 are some of the band combinations that have been proved to be useful for different geological purposes. The RGB 531 composite of the Landsat sub-scene in particular was found to be one of the best image in determining the boundaries and textures of the rocks in the study area, as shown in figure 3.

The general statistics and the correlation matrix values of the six ETM+ bands(1, 2, 3, 4, 5 and 7) are presented in tables 3 and 4, while the PCA transformation values are presented in table 5. The difference between the visible channels (bands 1, 2 and 3) and the infrared (IR) channels (bands 5 and 7) is demonstrated by PC2 in table 5.

Table 3. General statistics for the six studied Landsat 7 ETM+ bands in the Elaziğ Baskil area.

	Band 1	Band 2	Band 3	Band 4	Band 5	Band 6
Minimum	4.000	6.000	15.000	22.000	33.000	9.000
Maximum	122.000	162.000	146.000	108.000	87.000	114.000
Mean	52.279	69.910	60.121	49.400	52.028	56.128
Median	52.859	70.594	60.543	48.875	51.984	56.988
Std. dev.	17.204	21.400	17.131	10.720	7.373	13.831
Std. dev.(n–1)	17.204	21.400	17.131	10.720	7.373	13.831
Corr. eigenval.	5.409	0.313	0.201	0.049	0.016	0.012
Cov. eigenval.	1297.127	49.642	47.345	6.848	5.691	1.340

Table 4. Correlation matrix values for the six studied Landsat 7 ETM+ bands.

	Band 1	Band 2	Band 3	Band 4	Band 5	Band 7
Band 1	1.000	0.977	0.917	0.904	0.850	0.800
Band 2	0.977	1.000	0.913	0.897	0.833	0.857
Band 3	0.917	0.913	1.000	0.978	0.927	0.837
Band 4	0.904	0.897	0.978	1.000	0.964	0.823
Band 5	0.850	0.833	0.927	0.964	1.000	0.731
Band 7	0.800	0.857	0.837	0.823	0.731	1.000

Table 5. Covariance eigenvector values of the principal components (PCs) for the six studied Landsat 7 ETM+ bands.

	PC1	PC2	PC3	PC4	PC5	PC6
Band 1	0.466	−0.0455	0.156	−0.103	0.735	−0.029
Band 2	0.584	−0.266	0.444	0.138	−0.609	0.017
Band 3	0.460	0.132	−0.577	−0.606	−0.180	−0.197
Band 4	0.284	0.082	−0.413	0.360	0.039	0.781
Band 5	0.183	−0.006	−0.386	0.686	0.035	−0.588
Band 7	0.340	0.836	0.355	0.053	0.231	−0.060

Eigenvector loadings for PC2 of band 4 are not taken into account because of its approximation to zero (0.082). This PC2, which enhances the hydroxyl minerals, has higher loadings for bands 5 and 7, but with opposite signs. It has a negative contribution to band 5 (−0.006) and a positive contribution to band 7 (0.836). This indicates that the hydroxyl minerals would be dark pixels in the final hydroxyl image (figure 4). In order to display the areas with hydroxyl minerals in bright pixels, the negation of this PC2 should be taken into consideration (Tangestani and Moore 2000). A similar analysis of PC5 shows that the most important contributions come from band 1 (0.735) and band 3 (−0.180). This indicates that the iron oxide minerals will be bright pixels in the final iron oxide image (figure 5). According to Hunt *et al.* (1978), iron oxide will be mapped by bright pixels. An average of hydroxyl and iron oxide images can also be obtained. A false colour composite image with the hydroxyl image in red (R), the iron oxide image in green (G) and the average of

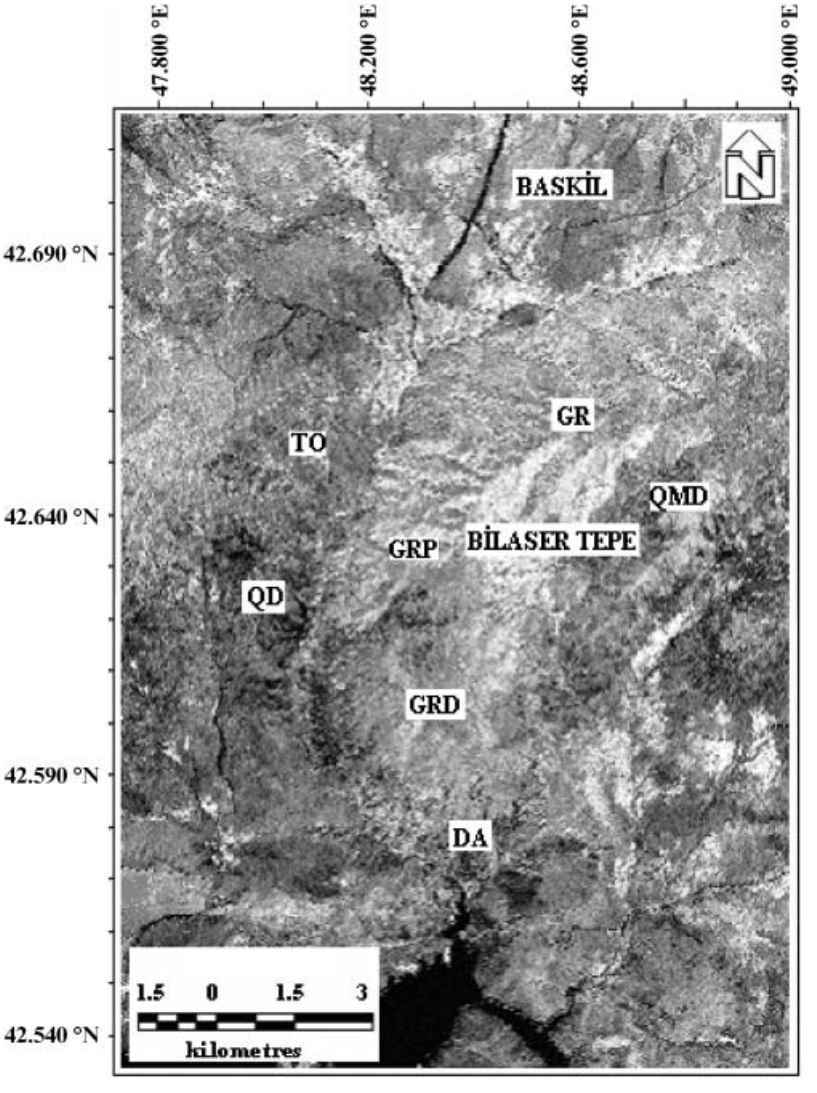

Figure 4. PC2 image of the hydroxyl minerals, showing the altered areas in dark pixels. All principal component transformations are made by using the six bands (1, 2, 3, 4, 5 and 7) of the Landsat 7 ETM+ data. (Abbreviations: GR – Granite, GRD – Granodiorite, GRP – Granite-porphyry, TO – Tonalite, QD – Quartz-diorite, QMD – Quartz-monzodiorite, DA – Dacite-porphyry.)

these two images in blue (B) is shown in figure 6. In the image, all intensely hydrothermally altered areas are shown in bright pixels.

The same technique can be applied by using two datasets each having four bands. For this purpose, two virtual datasets (1, 4, 5 and 7; 1, 3, 4 and 5) from Landsat 7 ETM+ bands are created. Statistics are calculated for each dataset, and covariance eigenvector values are examined. The transformation of the PCs on unstretched ETM+ bands 1, 4, 5 and 7 of the Elazığ-Baskil sub-scene is demonstrated in table 6. Bands 2 and 3 have been omitted on purpose in order to suppress iron oxide. The method followed for hydroxyl mapping during PCA on the four ETM+ bands (1, 4,

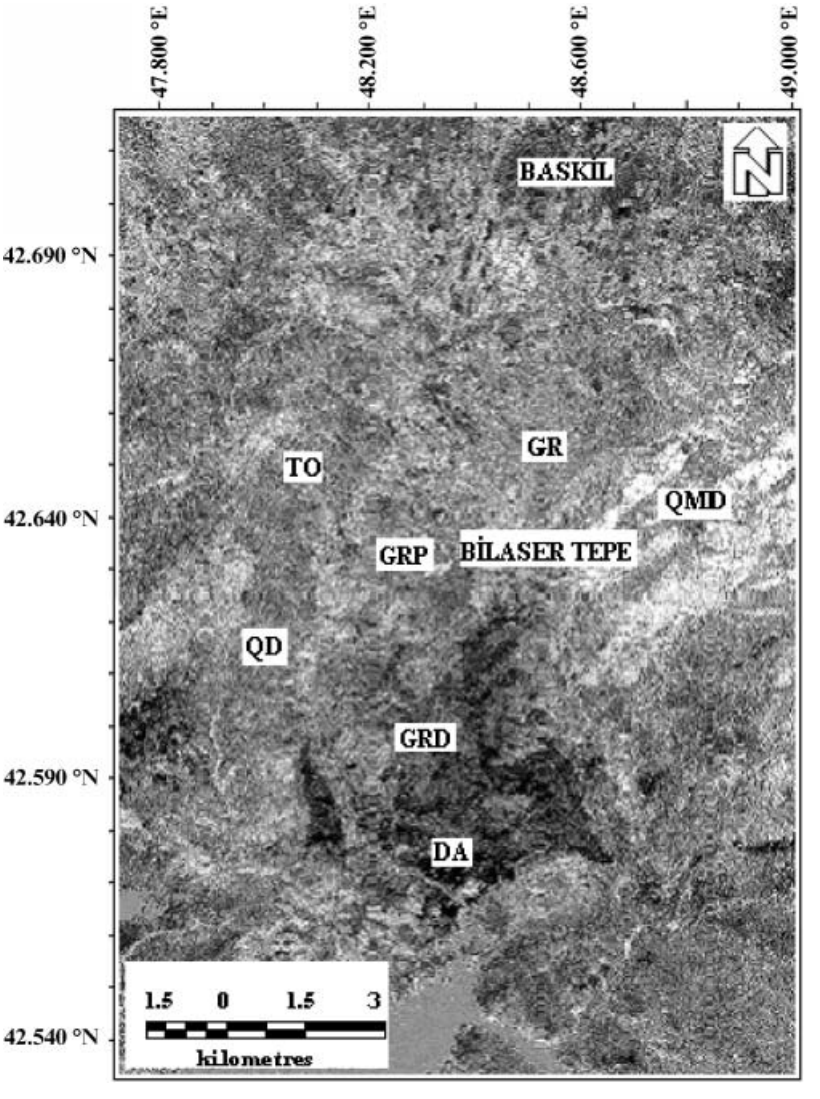

Figure 5. PC5 image of the iron oxide minerals, with the bright pixels showing the areas of iron oxide. All principal component transformations are made by using the six bands (1, 2, 3, 4, 5 and 7) of the Landsat 7 ETM+ data. (Abbreviations: GR – Granite, GRD – Granodiorite, GRP – Granite-porphyry, TO – Tonalite, QD – Quartz-diorite, QMD – Quartz-monzodiorite, DA – Dacite-porphyry.)

5 and 7) includes the analysis of the eigenvector loadings for bands 5 and 7 in the PC2 image. It is observed that the hydroxyl bearing minerals are distinguished better by a PC image with high or moderate eigenvector loadings for ETM+ 7, irrespective of sign, and high or moderate eigenvector loadings of the opposite sign for ETM+ 5. If there are dark pixels in the image obtained, these can be made brighter by negation of those PCs where the ETM+ 7 loadings are positive (Tangestani and Moore 2000).

For the first dataset (1, 4, 5 and 7 ETM+ bands), PC2 shows that the most important hydroxyl component contributions come from band 7 (0.846), whereas

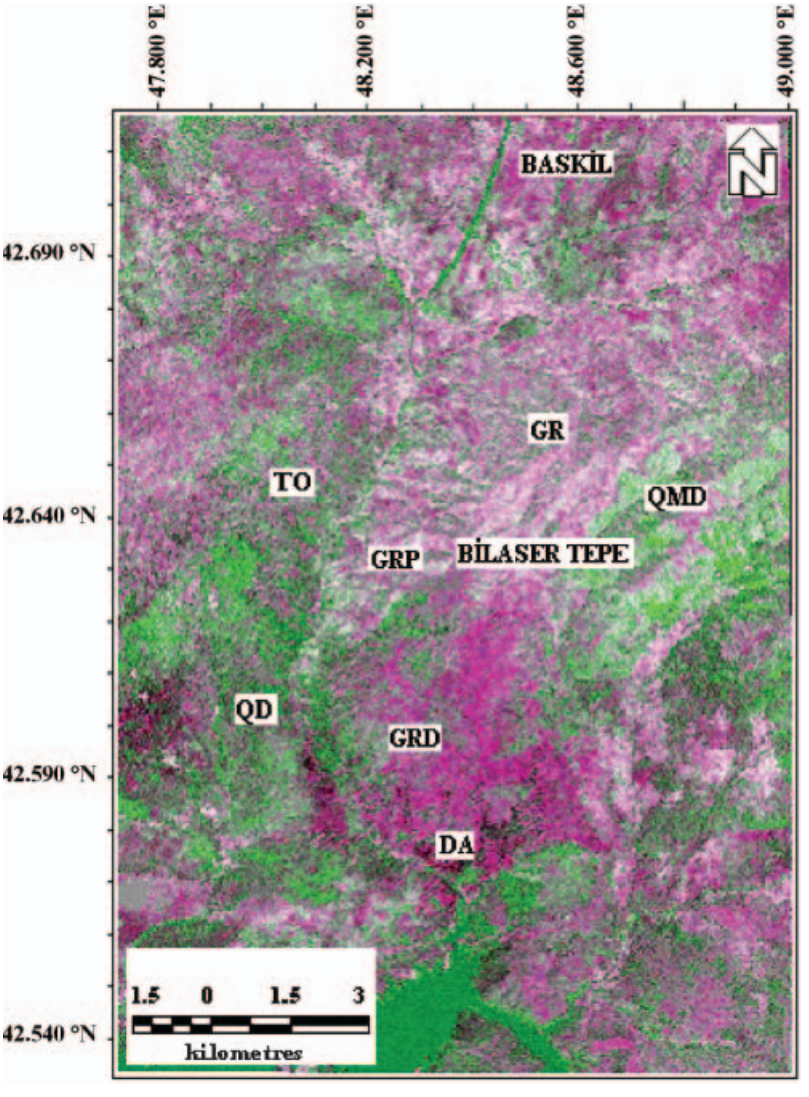

Figure 6. RGB composite image of the hydroxyl image(red band), the iron oxide image (green band) and the average of these two images (blue band).The highly altered areas are shown with bright pixels. All principal component transformations are made by using the six bands (1, 2, 3, 4, 5 and 7) of the Landsat 7 ETM+ data. (Abbreviations: GR – Granite, GRD – Granodiorite, GRP – Granite-porphyry, TO – Tonalite, QD – Quartz-diorite, QMD – Quartz-monzodiorite, DA – Dacite-porphyry.)

Table 6. Covariance eigenvector values of the principal components (PCs) of the first dataset (1, 4, 5 and 7 bands of Landsat 7 ETM+) for hydroxyl minerals.

	PC1	PC2	PC3	PC4
Band 1 (ETM 1)	0.690	−0.486	0.534	−0.050
Band 2 (ETM 4)	0.427	−0.125	−0.600	0.997
Band 3 (ETM 5)	0.274	−0.182	−0.589	−0.738
Band 4 (ETM 7)	0.518	0.846	0.092	−0.089

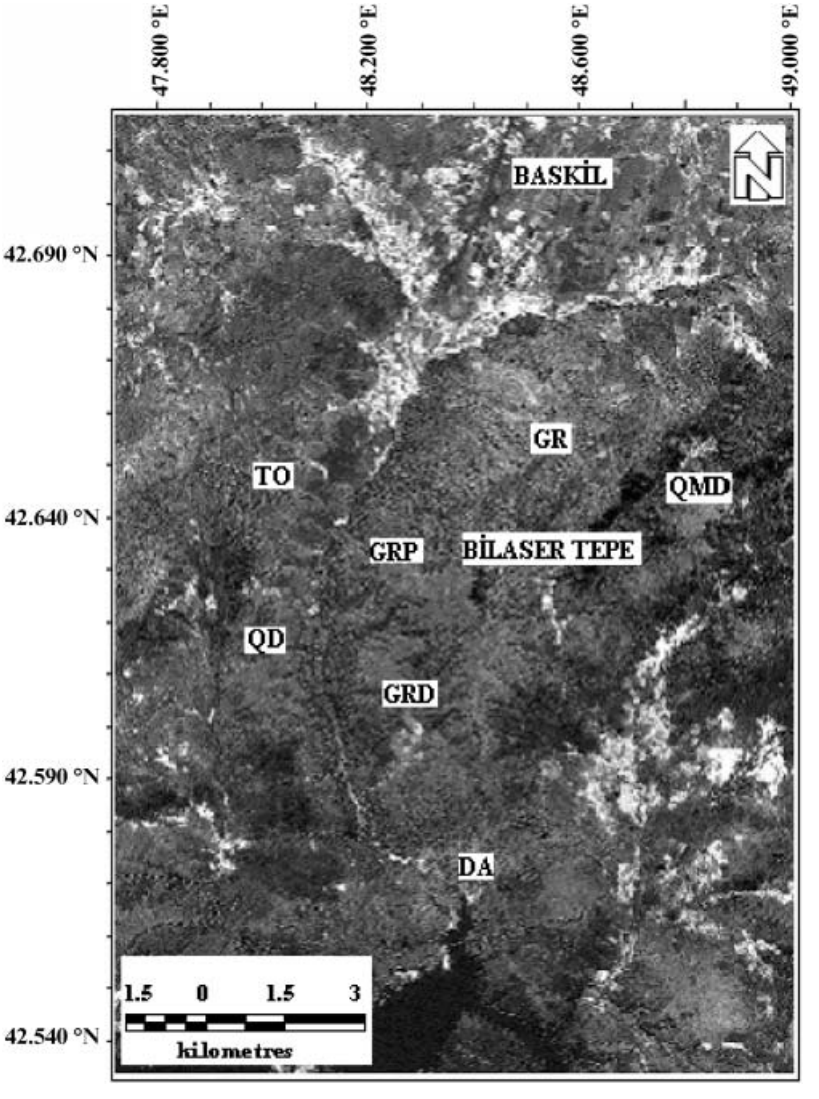

Figure 7. PC2 image of the hydroxyl component. Landsat 7 ETM+ bands (1, 4, 5 and 7) includes the analysis of the eigenvector loadings for bands 5 and 7 in the PC2 image. (Abbreviations: GR – Granite, GRD – Granodiorite, GRP – Granite-porphyry, TO – Tonalite, QD – Quartz-diorite, QMD – Quartz-monzodiorite, DA – Dacite-porphyry.)

loadings of band 5 have the opposite sign (−0.182). The 'hydroxyl image' of the Elazığ-Baskil area (shown in figure 7), obtained after the strong positive loadings for band 7 and low-moderate negative loadings for band 5, is an example supporting the above statement.

Table 7 displays the transformation of principal components on the four unstretched ETM+ bands 1, 3, 4 and 5 of the Elazığ-Baskil sub-scene. The rules for the iron oxide mapping shown in figure 8 are analogous to those of the hydroxyl mapping. Instead of bands 5 and 7 bands, this time bands 1 and 3 are of primary concern and the magnitude of the eigenvector loadings for these bands in the PCs should be moderate or strong with opposite signs. Table 7 gives the details of the

Table 7. Covariance eigenvector values of the principal components (PCs) of the second dataset (1, 3, 4 and 5 bands of Landsat 7 ETM+) for iron oxide minerals.

	PC1	PC2	PC3	PC4
Band 1 (ETM 1)	0.621	−0.778	−0.090	0.018
Band 2 (ETM 3)	0.629	0.439	0.594	0.243
Band 3 (ETM 4)	0.391	0.333	−0.338	−0.789
Band 4 (ETM 5)	0.256	0.301	−0.725	0.564

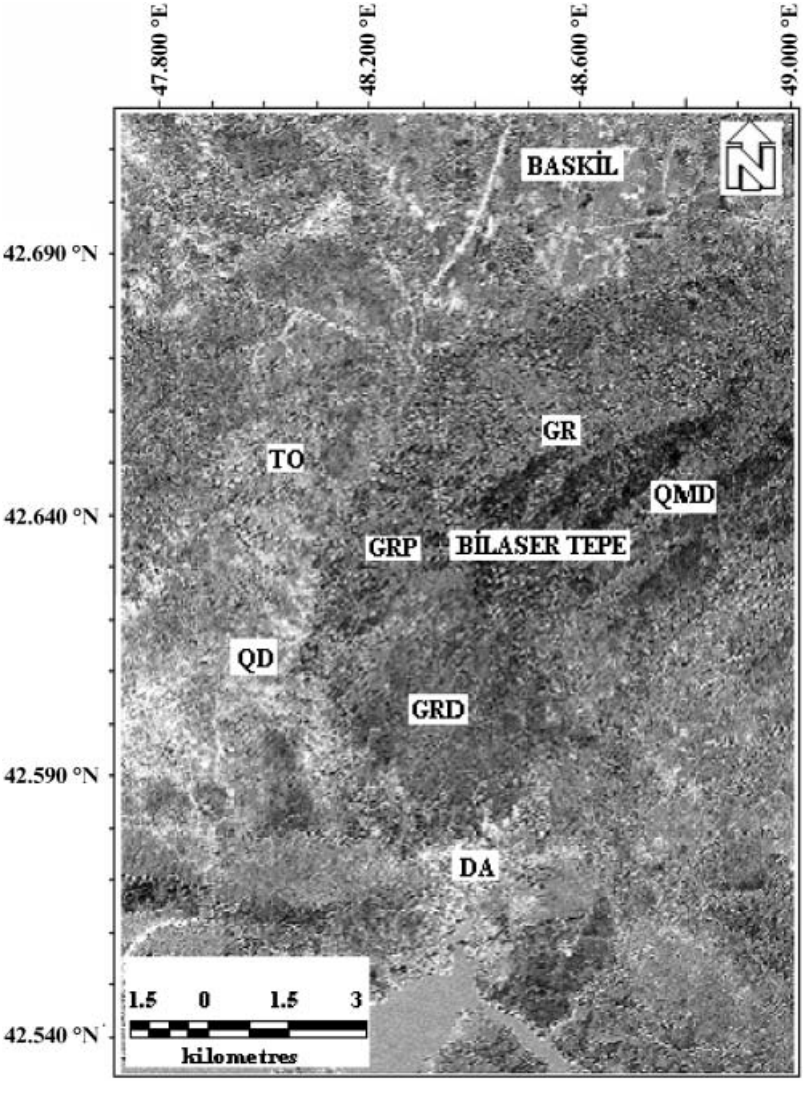

Figure 8. PC2 image of the iron oxide component. Landsat 7 ETM+ bands (1, 3, 4 and 5) includes the analysis of the eigenvector loadings for bands 1 and 3 in the PC2 image. (Abbreviations: GR – Granite, GRD – Granodiorite, GRP – Granite-porphyry, TO – Tonalite, QD – Quartz-diorite, QMD – Quartz-monzodiorite, DA – Dacite-porphyry.)

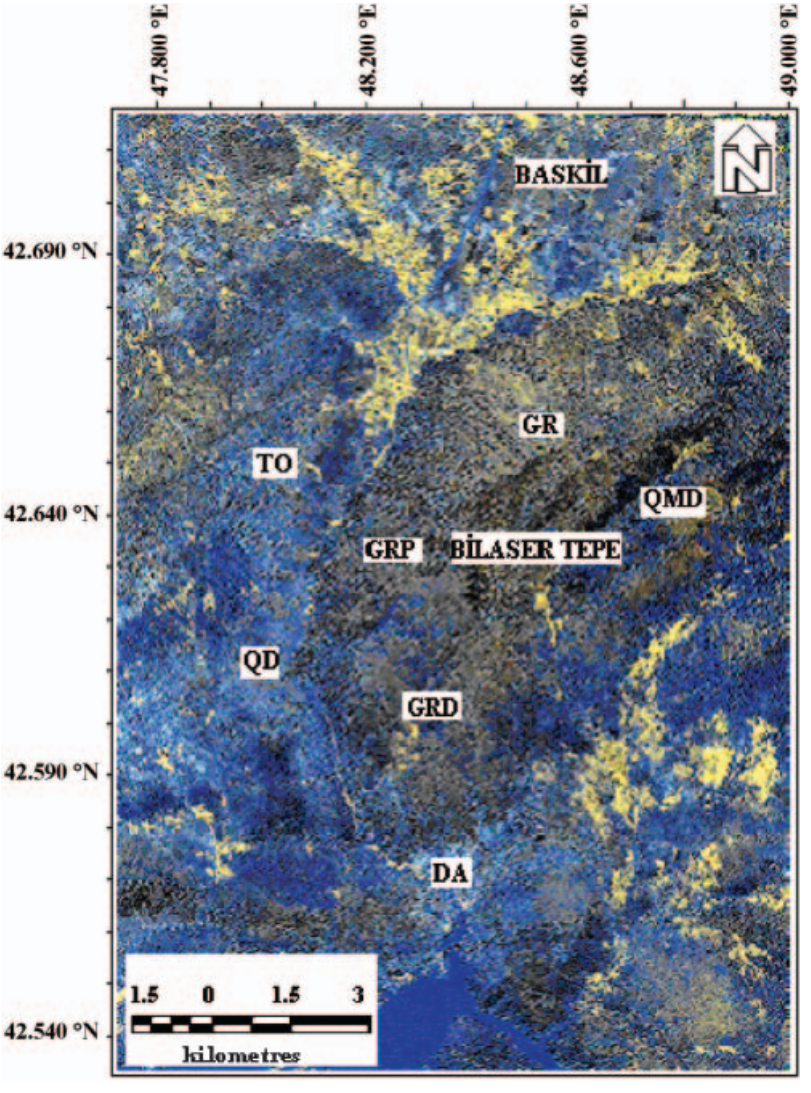

Figure 9. RGB composite of the hydroxyl component (red band), PC1 component (made of PC2 of hydroxyl image and PC2 of iron oxide image) (green band) and iron oxide component (blue band). (Abbreviations: GR – Granite, GRD – Granodiorite, GRP – Granite-porphyry, TO – Tonalite, QD – Quartz-diorite, QMD – Quartz-monzodiorite, DA – Dacite-porphyry.)

PC2, with moderate and positive loadings for band 3 (0.439) and strong, but negative, loadings for band 1 (−0.778).

PC1 is calculated from the two datasets of the four ETM + bands (1, 4, 5 and 7; 1, 3, 4 and 5). A false colour composite (RGB) image is shown with the hydroxyl component in red, the PC1 component in green and the iron oxide component in blue (figure 9).

4. Discussions

Modal mineralogical analysis provides information about the outer surface image of the rocks. The high amounts of felsic minerals (mainly alkali feldspars, plagioclase

and quartz) or dark coloured components (mainly hornblende, biotite, chlorite and opaque minerals) in the rocks have a direct effect on the image perceived by the satellite. An obvious example supporting this argument is the different reflectance values of felsic rocks and mafic rocks in the satellite image.

The modal mineralogical analysis explained in this paper is based on this idea. Initially, modal mineralogical analysis is applied to four samples from two different groups of rock types: the Baskil magmatites (dioritic rocks and tonalite) and the Bilaser Tepe magmatites (granite and granodiorite). Tables 1 and 2 showed the results for the Baskil and Bilaser Tepe magmatites.

Granular counting of minerals with a microscope in some rock thin sections has not been carried out in this process. There are several reasons for this decision: first of all, the dacite-porphyry samples are generally heavily altered; and secondly, the difference between the sizes of granules in granite-porphyry varies, thus the granular counting would not be reliable.

The difference in the results of the modal mineralogical analyses for the two magmatic rock types, and the difference between the altered minerals derived from these rocks had a significant impact on the mappings (hydroxyl and iron oxide) produced by using the Crosta technique.

The presence of coloured minerals, hornblende and chlorites are generally in high amounts in the Baskil magmatites (3.4% to 49.1%), whilst the light coloured rock forming minerals, such as alkali feldspar, plagioclase and quartz are of comparatively less amount (50.9% to 96.6%) in these rocks (table 1). Therefore, phyllic alteration is not widely seen in these rocks.

On the other hand, the Bilaser Tepe magmatites are rich in light coloured minerals (82.2% to 99.6 %) and poor in coloured rock forming mafic minerals (0.4% to 17.8 %) (table 2). Thus, during the hydrothermal alteration process, the hydroxyl group of minerals could have occurred much easily from alkali feldspar and plagioclases. As previously pointed out (Dumanlılar *et al*. 2005a, 2005b), phyllic, potassic and propylitic alteration types are widely seen in the Bilaser Tepe magmatites, while epidote-chlorite-carbonate alteration and a comparatively less amount of phyllic alteration were detected in the Baskil magmatites.

Baskil magmatites are seen in dark grey tones, whereas the Bilaser Tepe magmatites display relatively light grey to white colour in the hydroxyl image obtained (figure 4).

The total modal analysis percentage of the light coloured minerals of the tonalites of the Baskil magmatites are very high (93.75% to 96.9%) and display a very light coloured appearance in the RGB 531 composite (figure 3). On the other hand, the total modal percentage of the light coloured minerals in dioritic rocks are low (50.9% to 65.15%), but the total modal percentage of the coloured minerals are relatively high (34.5% to 49.1%), and they display a rather darker coloured appearance in the RGB 531 composite.

Iron-rich magmatic minerals such as biotite, hornblende and chlorites in magmatic rocks give a rather dark coloured image in the RGB 531 composite. Therefore, granite (Bilaser Tepe) and tonalite (Baskil) display rather light colour tones, whilst granodiorite(Bilaser Tepe), quartz-diorite (Baskil), quartz-monzodiorites (Baskil) show relatively darker colours in the RGB 531 composite.

Iron-rich mineral content of the Baskil magmatites display a lighter grey coloured appearance in the iron oxide image obtained (figure 5) in comparison with the Bilaser Tepe magmatites.

The alteration intensity differences of the Baskil and Bilaser Tepe magmatites are clearly shown in the final image obtained (figure 6). The lithological units of the Baskil magmatites (TO, QD, QMD) display green tones, whilst the colour of the units of the Bilaser Tepe magmatites (G, GP, GRD, GDP, DA) changes from dark magenta to very light magenta in this image (figure 6).

The alteration differences of these two magmatic groups were also tested with the Crosta technique using the two sets of four ETM + bands (1, 3, 4 and 5; 1, 4, 5 and 7). The iron oxide image (figure 8) created using the 1, 3, 4 and 5 bands, is found to be useful in differentiating the Baskil and Bilaser Tepe magmatites clearly, as it displays different grey tones. But, no obvious differences were obtained in the hydroxyl image (figure 7) created using 1, 4, 5 and 7 bands, of the studied magmatic groups. In the final R(hydroxyl) G(PC1) B(iron oxide) created from these two sets of four bands data, Baskil magmatites display dark to light blue tones, whilst the Bilaser Tepe magmatites display grey tones with the exception of the phyllic altered dasitic rocks, which gave light blue colours similar to the Baskil magmatites in the final RGB composite (figure 9).

Here are some of the examples that help to form a practical ground for the conclusions reached:

- The granitoid (GR) and granodioritic (GRD) rocks that form the Bilaser Tepe in the centre in figure 4 are in bright pixels when compared to the surrounding pixels that represent the Baskil magmatites (TO, QD, QMD).
- Similarly, these two magmatic groups can be differentiated using PC5. This time, the pixels in the centre become dark and the pixels around them become brighter (figure 5).
- On figure 6, in RGB format, the pixels representing the Bilaser Tepe magmatites have been displayed with magenta/dark magenta, while the Baskil magmatites are shown in different tones of green.
- The difference between these two types of rock groups can be made by looking at figures 8 and 9. The central pixels are dark grey in figure 8 and grey in figure 9, whereas the pixels representing the Baskil magmatites are light grey in figure 8 and blue in figure 9.

The following table shows a summary of the different colours for the Baskil and Bilaser Tepe magmatites (table 8).

In the light of all the results, it is possible to conclude that the Crosta technique is effective in the determination of the alteration types, as well as the magmatites of two different ages (phases), the Baskil and Bilaser Tepe rock groups, using six Landsat ETM + bands. The analysis performed using four ETM + bands is found to be a less effective differentiator between the two magmatites than the analysis using the six ETM + bands.

5. Conclusions

The use of satellite images and the application of the Crosta techniques on these data during the early stages of mineral exploration has been found to be very successful in delineating the hydrothermally altered rocks. Six and four bands of Landsat 7 ETM + data of December 2003 were used for enhancing the areas with hydroxyl and iron oxide minerals in the present study.

Principal component analyses were carried out on the six (1, 2, 3, 4, 5 and 7)and two sets of four ETM + bands(1, 3, 4 and 5; 1, 4, 5 and 7) and the relevant principal

Table 8. Characteristics of the two magmatites of the study area in various images.

	Bilaser Tepe magmatites	Baskil magmatites
Hydroxyl map from six band data (figure 4)	Bright	Dark
Iron oxide map from six band data (PC5)	Dark	Bright
RGB map from six band data (figure 6)	Magenta	Green
Iron oxide map from four band data component (figure 8)	Dark grey	Light grey
RGB map from four band data (figure 9)	Grey	Blue

components were chosen to obtain images that showed the areas enriched with iron oxide and hydroxyl minerals. The alteration differences of these two magmatic groups were also tested. It can be observed from the present study that the areas with potassic, phyllic, argillic and propylitic zones of alterations were enhanced much better by using the six bands of the Landsat 7 ETM+ data. However, no obvious differences were observed in the hydroxyl images of the magmatic groups studied with the Crosta technique using the four Landsat ETM+ bands 1, 4, 5 and 7. Baskil magmatites appeared as dark to light blue tones, whilst the Bilaser Tepe magmatites displayed grey tones in the RGB composite created from two sets of four band data; an exception to this was the phyllic altered dasitic rocks, which exhibited light blue colour, similar to the Baskil magmatites.

A close observation of the hydroxyl and iron oxide as well as the final RGB images created from the six bands (1, 2, 3, 4, 5 and 7) has shown that the Bilaser Tepe granitoids in the centre of the study area and the Baskil granitoids around them always appeared in different colours and shades. This observation leads to the fact that the Crosta techniques are not only effective in the generation of hydroxyl and iron oxide mappings, but are also effective in distinguishing two distinct magmatic groups that belong to different age groups and genesis.

Acknowledgements

Sincere thanks to Dr. Nilgün AYDAL for her help and support in various ways during the preparation of this paper. The authors would also like to express their sincere thanks to Emine Gökçe AYDAL (York University, UK) for reading the manuscript and giving valuable suggestions.

References

Abrams, M.J., Brown, D., Lepley, L. and Sadowski, R., 1983, Remote sensing for porphyry copper deposits in Southern Arizona. *Economic Geology*, **78**, pp. 591–604.

Akgül, M., 1991, Petrographical and petrological features of Baskil (Elazığ) granitoids. *Yerbilimleri Geosound*, **18**, pp. 67–78.

Akgül, B. and Bingöl, F.A., 1997, Petrographical and petrological features of magmatic rocks in the vicinity of Piran village (Keban). In *Proceedings of the Annual of Geological Engineering Department of the University of Selçuk*, Konya, Turkey, pp. 13–24.

ASUTAY, H.J., 1985, Geological and petrological investigation of around Baskil(Elazığ). PhD thesis, Ankara University Graduate School of Natural and Applied Sciences, Ankara, Turkey.

ASUTAY, H.J., 1988, Geology of the Baskil (Elazığ) area and petrology of Baskil magmatics. *Bulletin of Mineral Research and Exploration*, **107**, pp. 49–72.

ASUTAY, H.J. and TURAN, M., 1986, *Geology of the Keban-Baskil (Eastern Taurus)*. Report No: 8008, MTA (in Turkish).

BENNET, S.A., ATKINSON, W.W. and KRUSE, F.A., 1993, Use of thematic mapper imagery to identify mineralization in the Santa Teresa district, Sonara, Mexico. *International Geology Review*, **35**, pp. 1009–1029.

BEYARSLAN, M., 1991, Petrographical features of Ispendere Ophiolite (Malatya-Turkey). MSc thesis, Fırat University Graduate School of Science and Technology, Elazığ, Turkey.

BINGÖL, A.F., 1988, Petrographical and petrological featural setting on the intrusive rocks of Yüksekova Complex in the Elazig region (Eastern Taurus, Turkey). *Journal of Firat University*, **3**, pp. 1–17.

CROSTA, A. and MOORE, J.McM., 1989, Enhancement of Landsat thematic mapper imagery for residual soil mapping in SW Minais Gerais State, Brazil: a prospecting case history in Greenstone belt terrain. In *Proceedings of 7th ERIM Thematic Conference: Remote sensing for exploration geology*, pp. 1173–1187.

DRURY, S.A., 2001, *Image Interpretation in Geology,* Third edition, p. 304 (Blackwell Science Inc. (USA), Nelson Thornes (UK)).

DUMANLILAR, H., 1998, Investigation of mineralization around İspendere (Malatya). MSc thesis, Ankara University Graduate School of Natural and Applied Sciences, Ankara, Turkey, p. 132.

DUMANLILAR, H., AYDAL, D. and DUMANLILAR, Ö., 1999, Geology, mineralogy and geochemistry of sulphide mineralization of the Ispendere region (Malatya). *Bulletin of the Mineral Research and Exploration*, **121**, pp. 225–250.

DUMANLILAR, Ö., 1993, Geology and petrography of the magmatic rocks around İspendere (Malatya). MSc thesis, Ankara University Graduate School of Natural and Applied Sciences, Ankara, p. 62.

DUMANLILAR, Ö., 2002, Investigation of the mineralization related to the granitic rocks in Baskil (Elazığ). PhD thesis, Ankara University Graduate School of Natural and Applied Sciences, Ankara, Turkey, p. 196.

DUMANLILAR, Ö., AYDAL, D. and DUMANLILAR, H., 2005a, Baskil (Elazığ) Güneyindeki cevherleşmelerin jeolojik ve mineralojik özellikleri. *Jeoloji Mühendisliği Dergisi*, **29**, pp. 1–20. (Geological and mineralogical features of mineralizations from the southern part of Baskil (Elazığ). *Bulletin of Geological Engineering*, **29**, 1–20.).

DUMANLILAR, Ö., AYDAL, D., DUMANLILAR, H. and ALICI ŞEN, P., 2005b, Geological and geochemical characteristics of granitoids in the Eastern Tauride Belt. *International Geology Review*, Stanford, USA, accepted for publication.

HERECE, E., AKAY, E., KÜÇÜMEN, E. and SARIASLAN, M., 1992, *Geology of Elazığ- Sivrice-Palu region*, unpublished report no: 9634, MTA (in Turkish).

HUNT, G.R., SALISBURY, J.W. and LENHOFF, G.J., 1978, Visible and near-infrared spectra of minerals and rocks: III Oxides and hydroxides. *Modern Geology*, **2**, pp. 195–205.

KAUFMAN, H., 1988, Mineral exploration along the Agaba-Levant structure by use of TM-data concepts, processing and results. *International Journal of Remote Sensing*, **9**, pp. 1630–1658.

LOUGHLIN, W.P., 1991, Principal component analysis for alteration mapping. *Photogrammetric Engineering and Remote Sensing*, **57**, pp. 1163–1169.

LOWELL, J.D. and GUILBERT, J.M., 1970, Lateral and vertical alteration-mineralization zoning in porphyry ore deposits. *Economic Geology*, **65**, pp. 373–408.

PERINÇEK, D., 1979, *The Geology of Hazro-Korudağ-Çüngüş-Maden-Ergani-Hazar-Elazığ-Malatya Area: Guide Book*, Türkiye Jeoloji Kurumu Yayını, p. 33.

RANJBAR, H., HONARMAND, M. and MOEZIFAR, Z., 2004, Application of the Crosta technique for porphyry copper alteration mapping using TM+ data in the southern part of the Iranian volcanic sedimentary belt. *Journal of Asian Earth Sciences*, **24**, pp. 237–243.

RANJBAR, H., HONARMAND, M., MOEZIFAR, Z. and ILAGHI, O., 2002, Integration and analysis of remote sensing, airborne geophysics and geochemical data of Shar Cheshmeh area, using directed principal component analysis. In *9th International Remote Sensing Conference*, 23–26 September 2002, Agia Pelagia, Greece, pp. 429–437.

RUTZ-ARMENTA, J.R. and PROL-LEDESMA, R.M., 1998, Techniques for enhancing the spectral response of hydrothermal alteration minerals in Thematic Mapper images of Central Mexico. *International Journal of Remote Sensing*, **19**, pp. 1981–2000.

SABINS, F.F., 1997, *Remote Sensing Principles and Interpretation*, p. 494 (New York: W.H. Freeman).

SABINS, F.F., 1999, Remote sensing for mineral exploration. *Ore Geology Reviews*, **14**, pp. 157–183.

TANGESTANI, M.H. and MOORE, F., 2000, Iron oxide and hydroxyl enhancement using the Crosta Method: a case study from the Zagros Belt, Fars province, Iran. Communication. *JAG*, **2**, pp. 140–146.

TANGESTANI, M.H. and MOORE, F., 2001, Comparison of three principal component analysis techniques to porphyry copper alteration mapping. A case study, Meiduk area, Kerman, Iran. *Canadian Journal of Remote Sensing*, **27**, pp. 176–182.

TURAN, M., 1984, The stratigraphy and tectonic of the Baskil-Aydınlar (Elazığ). PhD thesis, Fırat Universitesi, Graduate School of Science and Technology, Elazığ, Turkey, p. 180.

TURAN, M., AKSOY, E. and BINGÖL, F.A., 1995, The features of geodinamic evolution of the Eastern Taurides in Elazığ region: Fırat Universitesi, Fen ve Müh. *Bilimleri Dergisi*, **7**, pp. 177–199 (in Turkish).

YAZGAN, E., 1981, Study of active paleo-continent margin in Eastern Taurides (Upper Cretaceous–Middle Eocene). *Hacettepe Univ. Yerbilimleri*, **7**, pp. 83–104.

YAZGAN, E., 1984, Geodynamic evolution of the Eastern Taurus region. In *Proceedings of Geology of the Taurus belt*, O. Tekeli and M.C. Göncüoğlu (Eds), MTA, Ankara.

YAZGAN, E., ASUTAY, H.J., GÜLTEKIN, M.C., POYRAZ, N., SIREL, E. and YILDIRIM, H., 1987, *Geology of the southeastern Malatya and geodynamic evaluation of Eastern Taurides*, unpublished report no:2268, MTA (in Turkish).

YAZGAN, E. and CHESSEX, R., 1991, Geology and tectonic evolution of the Southeastern Taurides in the region of Malatya. *Türkiye Petrol Jeologları Dergisi Bülteni*, **3**, pp. 11–42 (in Turkish).